Evolution of Sensitivity Directions during Autoignition

Weiqi Ji [a], Zhuyin Ren [a,*], Chung K. Law [a,b]

[a] *Center for Combustion Energy, Tsinghua University, Beijing 100084, China*

[b] *Department of Mechanical and Aerospace Engineering,*

Princeton University, Princeton, NJ 08544, USA

***Corresponding Author:** zhuyinren@mail.tsinghua.edu.cn

Colloquium: Gas-phase Reaction Kinetics

Total Length: 6180 words (Method 1)

Listing in detail:

Main text: 3482 words (Introduction 994+ body 2148 + conclusion 326+ acknowledgments 14)

Equations: 106 words, i.e., (14)*7.6x1 = 106

References: 507 words, i.e., (27+2)*2.3*7.6=402

Tables: 122 words, i.e., (6+2)*7.6*2=122

Figures: 1963 words, i.e.

Fig.1=(50+10)*2.2*2+41=305; Fig.2=(50+10)*2.2*2+17=281;

Fig.3=(95+10)*2.2*2+12=194; Fig.4=(107+10)*2.2+10=267;

Fig.5=(70+10)*2.2+19=371; Fig.6=(55+10)*2.2+27=170;

Fig.7=(70+10)*2.2+23=375;

Supplemental material: available

Abstract

Sensitivity analysis of the ignition delay time and species profiles to kinetic parameters has been widely used to identify the rate-limiting steps during the autoignition process, providing insights for the optimization of the reaction mechanism. This work studies the time evolution of the sensitivity directions of the temperature and species concentration during autoignition. The direction is represented by a unit vector along the gradient of the simulation output to the kinetic parameters, and the alignment between the two directions are measured by the inner product between the corresponding unit vectors. We use evolution of the sensitivity directions to reveal changes in the rate-limiting steps and the correlation among species at different phases of the ignition delay period. It is found that the sensitivity directions of temperature and the concentrations of the major intermediate species are similar to each other during the entire ignition delay period. In particular, they converge to the same direction when approaching the ignition state, and the direction is the same as the one for the ignition delay time. The correlation is validated for various fuels across a wide range of pressures and temperatures, and works for both single-stage ignition and two-stage ignition. Consequently the sensitivity of the ignition delay time can be efficiently evaluated based on the temperature sensitivity at the ignition point, for which a single run of the simulation can produce the sensitivity to all parameters, as otherwise the sensitivity of the ignition delay time has to be evaluated through finite difference, in which the number of runs equals to the number of parameters. It can also significantly reduce the computation cost of gradient-based algorithms for the purpose of mechanism optimization and uncertainty quantification.

Keywords: Ignition delay time; sensitivity analysis; sensitivity direction; similarity; gradient

1. Introduction

Autoignition of hydrocarbon fuels has been extensively studied for engine design and the development and validation of kinetics mechanisms. The ignition delay time (IDT), which is the time for the induction period before rapid heat release, is of primary importance and is readily measurable using rapid compression machines and shock tubes. It has also been routinely simulated with detailed reaction mechanisms, in which the kinetic parameters could have pronounced effect on the predicted IDT. The sensitivity of IDT to the rate constants can reveal the rate-limiting steps controlling the ignition process and provide valuable insights into the mechanism optimization.

While sensitivity analysis of IDT has become a standard procedure for mechanism development, insufficient attention has been directed to the evolution of the sensitivities of composition (e.g., species concentrations and temperature) with respect to kinetic parameters during autoignition. In this work, we study the sensitivities to the pre-exponential "A-factors" in the Arrhenius reaction rate expressions. The governing ordinary differential equations (ODEs) for composition evolution during the auto-ignition process are of the general form

$$\frac{d\boldsymbol{\varphi}}{dt} = \boldsymbol{F}(\boldsymbol{\varphi}, t; \boldsymbol{k}), \tag{1}$$

where $\boldsymbol{\varphi}(t)$ is the composition vector consisting of species mass fractions and temperature, and $\boldsymbol{k}$ is the vector of reaction rate constants. The first-order sensitivity coefficients are defined as

$$S_{ij} = \frac{\partial \varphi_i}{\partial k_j}, \tag{2}$$

with the evolution equations being

$$\frac{dS_{ij}}{dt} = \frac{\partial \boldsymbol{F}}{\partial \boldsymbol{\varphi}} S_{lj} + \frac{\partial F_i}{\partial k_j}. \tag{3}$$

The corresponding sensitivity matrix $\boldsymbol{S}(t)$, of sizes $n_c \times n_r$, evolves with time and depends on the local composition, with n_c being the dimension of the composition and n_r the number of kinetic parameters. The kinetic parameters here refer to the pre-exponential "A-factors" of the n_r elementary

reactions, and the *i*th row of $\boldsymbol{S}(t)$ represents the sensitivity vector of the *i*th composition variable in the n_r-dimensional parameter space, with its magnitude and direction evolving with time. The relative importance of the kinetic parameters is revealed by the individual components of the sensitivity vector.

Various interpretations of the time-evolving sensitivity vectors have been proposed, such as measuring the averaged sensitivity over a certain time range [1, 2]. For example, Vajda *et al.* [2] employed principal component analysis (PCA) on $\boldsymbol{S}(t)$ over a time interval, *i.e.*, eigen decomposition of $\int_{t_1}^{t_2} \boldsymbol{S}^T \boldsymbol{S} \mathrm{dt}$, to reveal the sensitive reactions and the coupling between the reactions. The principal components, referred to the eigenvectors with large eigenvalues, are linear combinations of the kinetic parameters, along which the predicted composition profiles mostly change.

Turányi and co-workers [3-7] have systematically studied three types of similarity among the sensitivity vectors during autoignition, i.e., (i) *Local similarity*: the ratio S_{im}/S_{jm} is the same for any parameter k_m. (ii) *Scaling relation*: the ratio S_{im}/S_{jm} is equal to $\frac{\partial \varphi_i}{\partial t} / \frac{\partial \varphi_j}{\partial t}$. (iii) *Global similarity*: the ratio $S_{in}(t)/S_{im}(t)$ does not change with *t* within the interval (t_1, t_2). Similar patterns are also observed in laminar flames and in models of biological problems [8].

This work also focuses on the patterns among the sensitivity vectors during auto-ignition. While previous work have studied the similarity for hydrogen and methane with single-stage ignition, this work shall extend the study to large hydrocarbon fuels with two-stage ignition. More importantly, while the correlation between the sensitivity vector of laminar flame speed and that of the local composition sensitivity has been studied in [3-7], it is unclear how the sensitivity vector of the IDT is related to the local composition sensitivity. Here, we shall show that the sensitivity vector of IDT and the local temperature sensitivity at the instance of ignition are parallel, which provides the possibility to evaluate the sensitivity of IDT based on the composition sensitivity. The composition sensitivities are usually obtained by solving the governing equations for the sensitivity matrix during the

autoignition integration. Although the computational cost increases with the number of kinetic parameters in the current implementation of legacy combustion codes such as Chemkin [9] and Cantera [10], it can be reduced to be independent of the number of parameters and is comparable to a single run of the autoignition integration via the adjoint method [11]. Then the sensitivity of any other quantities defined as the integral of the solution variables can be readily computed by matrix manipulation. However, since IDT is defined as the time instant when the temperature profile reaches its inflection point, its sensitivity is usually evaluated through brute force finite difference approach, for which the kinetic parameters are perturbed one by one. Consequently the number of autoignition integrations required is equal to n_r and the computational cost becomes very expensive for large hydrocarbon fuel with thousands to tens of thousands of reactions.

To alleviate the computational cost, we propose an efficient approach for computing the sensitivity of IDT by exploiting the correlations between the sensitivities of IDT and composition. By doing so, the computation of the sensitivity of IDT only requires two runs, and the cost can be comparable to that for the autoignition integration using the adjoint method [11]. Then the computational cost for statistical calibration of the reaction mechanism [12, 13], construction of the response surface for the kinetic parameters [12, 14], and global sensitivity analysis [15] can be significantly reduced by taking advantage of various gradient-based algorithms, such as those of steepest descent method, active subspace [14, 16, 17] and so on. For example, in [14], with the sensitivities of IDT, the active subspace method is employed to identify one-dimensional active subspaces in the 33 and 217-dimensional uncertain kinetic parameter space for the IDT of hydrogen/air and methane/air mixtures, respectively. Then the cost of subsequent construction of response surface and global sensitivity analysis is reduced by several orders. With the above efficient approach for computing the gradient of IDT, the total cost will be further reduced and the speed up factor is proportional to the number of reactions.

In the following, we shall first investigate the similarity in the evolution of the sensitivity directions in both single-stage ignition and two-stage ignition. We then show that the sensitivity vector of IDT is parallel to the composition sensitivity vector at the instant of ignition. Finally, an efficient approach for computing the sensitivity of IDT based on the correlation is proposed and validated.

2. Evolution of composition sensitivity

Equations (1) and (3) are integrated together using Cantera to obtain the evolution of both composition and sensitivities. The normalized composition sensitivity is given by $\widetilde{S_{ij}} = \frac{k_j}{\varphi_i}\frac{\partial \varphi_i}{\partial k_j}$. For the sensitivity vector of the *i*th composition variable, *e.g.*, $\widetilde{\boldsymbol{S}_i} \equiv \left[\widetilde{S_{i1}}, \ldots, \widetilde{S_{in_r}}\right]^{\mathrm{T}}$, its direction is the same as that of the unit vector $\boldsymbol{u}_i \equiv \widetilde{\boldsymbol{S}_i}/\left\|\widetilde{\boldsymbol{S}_i}\right\|_2$ and its magnitude is given by $\lambda \equiv \left\|\widetilde{\boldsymbol{S}_i}\right\|_2$.

In this study, the ignition state is defined as the time instant of the maximum heat release rate. The mechanisms employed are summarized in Table 1. While the methane mechanism involves only high-temperature chemistry and single-stage ignition, the other three fuels involve low-temperature chemistry and may result in two-stage ignition. Detailed mechanisms are used for methane and DME, while skeletal mechanisms are used for n-heptane and *iso*-octane to reduce the computation cost of finite difference approach. The autoignition simulation is performed under constant volume; constant pressure simulation leads to the same conclusion and hence is not shown here.

Table 1. Chemical mechanisms and conditions for the autoignition processes

Fuel/mech	**No. species**	**No. reactions**	$\boldsymbol{\phi}$	p **[atm]**	T **[K]**
Methane (CH_4) **[18]**	53	325	0.5, 1, 2	1, 20	1000-1500
DME (CH_3OCH_3) **[19]**	55	290	0.5, 1, 2	1, 20	1000-1500
n-heptane (n-C_7H_{16}) **[20]**	88	729	0.5, 1, 2	1, 20	600-1500
iso-octane (i-C_8H_{18}) **[21]**	143	1178	0.5, 1, 2	1, 20	600-1500

Representative evolution profiles of the magnitude of the temperature sensitivity vector as well as the rate-of-change of temperature are shown in Fig. 1. Time is normalized by the ignition delay time and is denoted as NT. As expected, the magnitude of the temperature sensitivity vector changes simultaneously with the rate-of-change of temperature, which remains relatively small and increases dramatically near the ignition point.

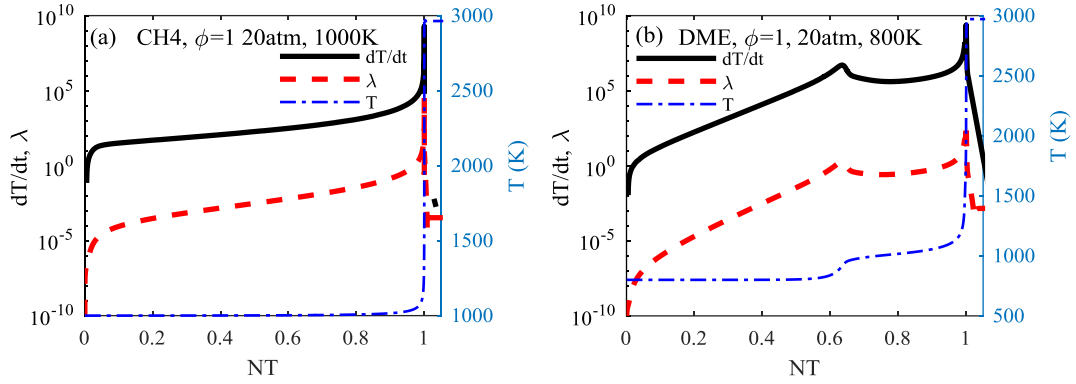

Fig. 1. Evolution of temperature, its rate of change, and the magnitude of its sensitivity vector to kinetic parameters against the normalized time. The unit of dT/dt is K/s. The IDT is 38.4 ms in (a) and 0.7 ms in (b).

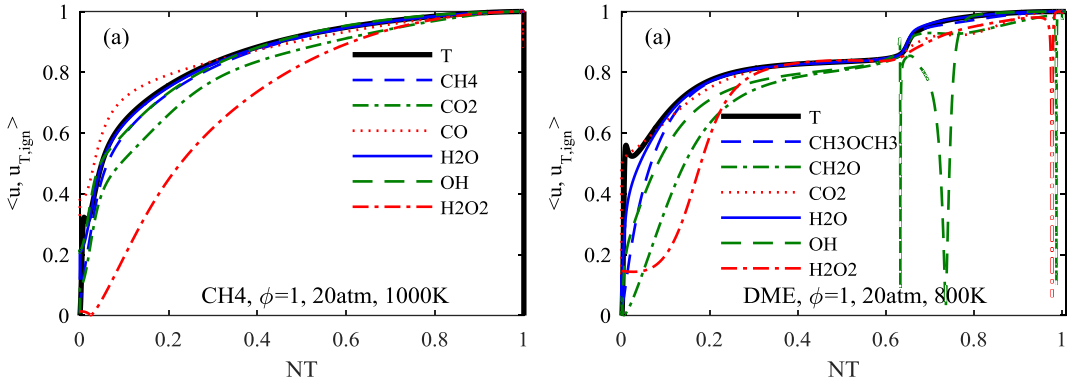

Fig. 2. Evolutions of the inner product (absolute value) between the sensitivity directions of composition and $\boldsymbol{u}_{T,ign}$.

Figure 2 shows evolution of the sensitivity directions of temperature and several major intermediate species for methane and DME. The profiles for *n*-heptane and *iso*-octane with two-stage ignition are similar to DME and are provided in the supplemental material. To facilitate the comparison,

the inner product $< \boldsymbol{u}_i(t), \boldsymbol{u}_{T,ign} >$ is employed to represent the angle between the directions of the composition sensitivities and that of temperature sensitivity at the ignition point, with $< \boldsymbol{u}_i(t), \boldsymbol{u}_{T,ign} >= \pm 1$ representing perfect alignment. For methane with single-stage ignition, it is shown that the temperature sensitivity direction quickly aligns with $\boldsymbol{u}_{T,ign}$, with an inner product of 0.90 at NT = 0.5, and 0.99 at NT = 0.9. For DME with two-stage ignition, two-stage alignments of the temperature sensitivity vector are observed, corresponding to the first and second stage ignition. It quickly aligns with $\boldsymbol{u}_{T,ign}$ with an inner product of 0.95 at NT = 0.7, and 0.99 at NT = 0.9. Therefore, the global similarity defined in [3] is observed where approaching ignition for both the first and second stage ignition.

It is also shown that the sensitivity directions of the fuel, the final products CO_2, H_2O and the major intermediate species CO, OH change simultaneously along the temperature sensitivity direction, which corresponds to the local similarity defined in [3]. Furthermore, the directions of species sensitivities and temperature sensitivity are largely correlated with each other, although deviations are observed for the species CH_2O, H_2O_2 and OH in the DME case. Note that the absolute value of the inner product is presented in Fig. 2, and the sign for the inner product between OH sensitivity and the reference direction changes due to its negative net production rate during the transition from the first stage to the second stage ignition. Typical evolution of the OH profile during the transition can be found in [22]. During the later phases of the second stage ignition, the sign is reversed to be positive as the OH concentration increases again. The same reason accounts for the behavior of H_2O_2 and CH_2O near the second stage ignition. Nevertheless, all the composition sensitivity vectors evolve toward aligning with $\boldsymbol{u}_{T,ign}$ when approaching the ignition state.

Zsely *et al.* [9] have shown that the similarity of sensitivity functions is related to the existence of low-dimensional manifolds in chemical kinetic systems; they are briefed here for the later discussion

on the correlation between the ignition delay time and local temperature sensitivity. In the composition space, the one-dimensional trajectory from autoignition quickly approaches the attracting manifold. König and Maas [23] showed that the sensitivity of the attracting manifold to rate constants vanishes and the sensitivity of a trajectory to rate constants only has a component parallel to the attracting manifold when approaching equilibrium. At the ignition state, if the attracting manifold is one-dimensional and its sensitivity vector to rate constants is predominantly in the tangential direction of the manifold, then the responses of different composition components to the rate constants are also parallel with each other and this explains the alignment of the species sensitivity directions. As shown in Fig. 1a, the temperature sensitivity remains relatively small throughout the induction period and then increases dramatically near the ignition point. It is anticipated that when approaching the ignition state, temperature is insensitive to those sensitive reactions for the induction period and its evolution and sensitivity (including direction and magnitude) is dominated by the local kinetics around the ignition state. This explains why the direction of temperature sensitivity reaches a plateau when approaching ignition.

Next, we shall investigate evolution of the sensitive reactions as revealed by the components of $\boldsymbol{u}_{T,ign}$. Figure 3a shows the most sensitive reactions for temperature at the ignition point for the stoichiometric methane/air mixture at 20 atm and 1000K. The reactions of $CH_3+HO_2=CH_3O+OH$ (R119), $CH_2O+O_2=HCO+HO_2$ (R32) and $CH_3+O_2=HCO+HO_2$ (R156) are the most sensitive chain branching reactions while $2CH_3(+M)=C_2H_6(+M)$ (R158) and $2HO_2=H_2O_2+O_2$ (R116) are the most chain termination reactions. Evolution of the corresponding components is then shown in Fig. 4a. It is seen that during the initial stage, the major competition occurs between R156 and R158 in consuming the CH_3 radical, which is consistent to the rate of production analysis (ROP) in [24]. Then the sensitivity of R156 gradually decreases relative to R119, which is attributed to the shift of equilibrium

due to the increasing CH_2O concentration [24].

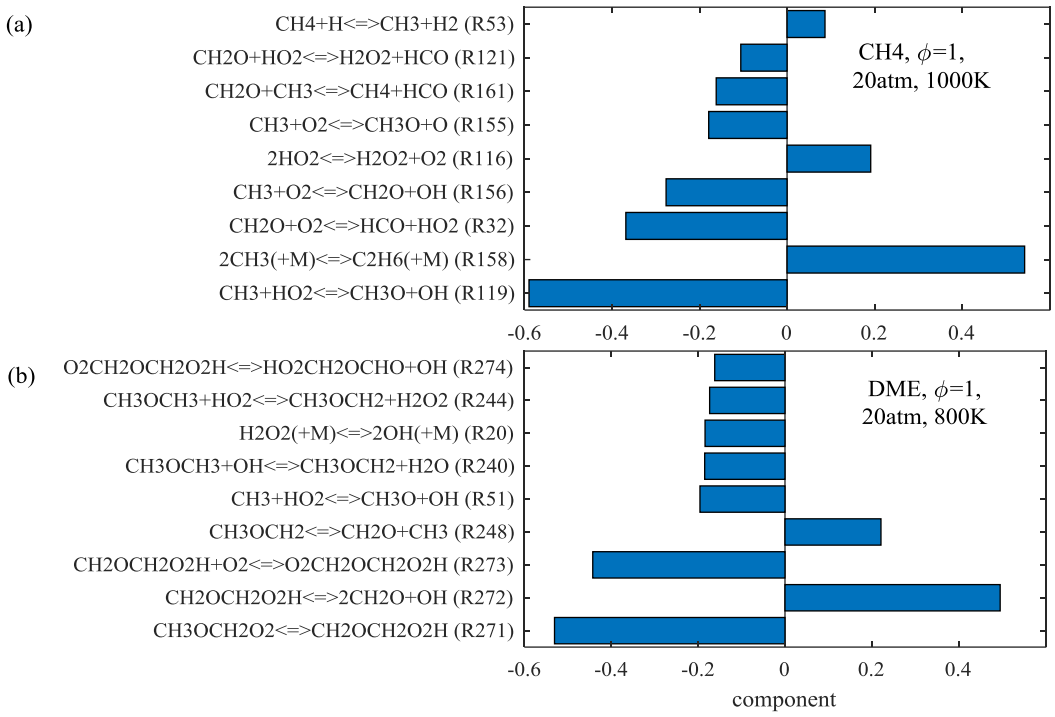

Fig. 3. The most sensitive reactions for temperature at the ignition point.

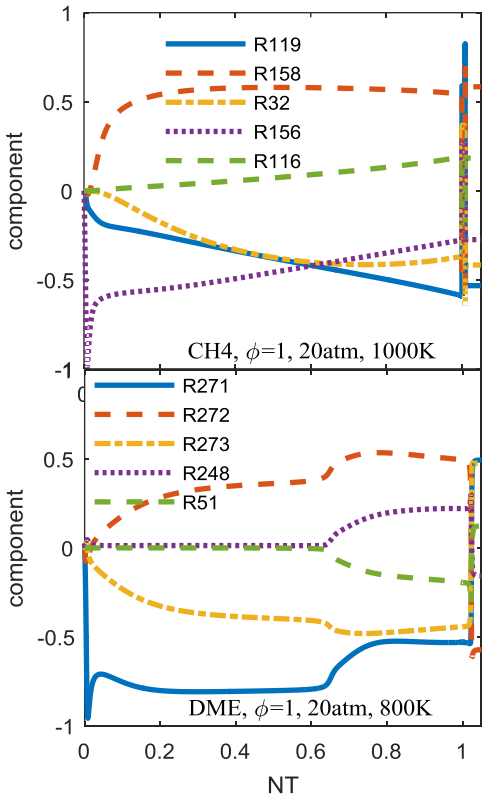

Fig. 4 Evolution of the most sensitive reactions for temperature.

Regarding the case of DME with two-stage ignition as shown in Fig. 3b, the most sensitive

reactions for temperature at the ignition point are $CH_3OCH_2O2=CH_2OCH_2O2H$ (R271), $CH_2OCH_2O2H=2CH_2O+OH$ (R272), $CH_2OCH_2O2H+O_2=O_2CH_2OCH_2O2H$ (R273) and $CH_3OCH_2=CH_2O+CH_3$ (R248). The isomerization reaction R271 and the second oxygen addition reaction R273 are the key steps leading to low-temperature chain branching reactions. Reactions R272 and R248 are the β-scission reactions competing with the low-temperature chain branching reactions. Their evolutions in Fig. 4 show that R271 is dominant during the initial stage of the induction period. With increasing concentration of CH_3OCH_2O2 and CH_2OCH_2O2H, the relative sensitivities of R272 and R273 gradually increase and approach a plateau when approaching the first stage ignition point. After the temperature increases during the first stage ignition, β-scission of the fuel radical, R248, and the subsequent reaction R51, which are well known to be important in the intermediate-to-high temperature regime [25, 26], start to be important. Interestingly, the relative sensitivity of R271 is significantly reduced, while the sensitivity of the other key low-temperature reactions, R272 and R273, are promoted. This is possibly a consequence of R271 reaching partial equilibrium and the net reaction rate is then determined by the subsequent rate-limiting steps, such as R272 and R273.

In short, we have demonstrated that evolution of the composition sensitivity can help analyze the corresponding evolution of the rate-limiting steps during the ignition delay period. The similarity among the sensitivity vectors observed in previous work [3] have been extended to both the first and second stage ignition, i.e., (I) The sensitivity for temperatures and most of the species concentrations are largely correlated with each other. (II) The sensitivity directions for the major intermediate species concentration and temperature align with each other when approaching the ignition state. Next, we shall study the correlations between the sensitive directions of composition and the ignition delay time.

3. Efficient approach for computing the sensitivity of IDT

The normalized sensitivity of the ignition delay time τ is defined as

$$\widetilde{S_{\tau,i}} = \frac{k_i}{\tau}\frac{\partial \tau}{\partial k_i} = \frac{\partial \ln \tau}{\partial \ln k_i} \tag{4}$$

Similarly, the sensitivity direction for IDT is the same as the unit vector $\boldsymbol{u}_\tau \equiv \widetilde{\boldsymbol{S}_\tau}/\left\|\widetilde{\boldsymbol{S}_\tau}\right\|_2$. The sensitivity of IDT can be evaluated via the finite difference approach with a perturbation factor, *e.g.*, $\delta = 5\%$, i.e.,

$$\widetilde{S_{\tau,i}} \approx \frac{\ln \tau((1+\delta)k_i) - \ln \tau(k_i)}{\ln(1+\delta)} \tag{5}$$

The perturbation factor is chosen to be large enough to avoid numerical noise (discretization error) in computing IDT, and small enough to avoid nonlinear effects.

It is found that the direction of sensitivity for IDT and temperature sensitivity at ignition are almost the same, *i.e.*, $\boldsymbol{u}_\tau$ aligns with $\boldsymbol{u}_{T,ign}$. $\boldsymbol{u}_{T,ign}$ is the sensitivity vector of temperature at the ignition point with respect to the kinetic parameters. The level of alignment is also assessed by the inner product between the two sensitivity directions, which is larger than 0.999. The largest 25 components (in magnitude) of the unit vector $\boldsymbol{u}_\tau$ for the stoichiometric mixture of methane/air under the pressure of 20 atm and initial temperature of 1000 K are shown in Fig. 5. Also shown are the component-wise relative difference between $\boldsymbol{u}_\tau$ and $\boldsymbol{u}_{T,ign}$, defined as $\boldsymbol{\epsilon_i} \equiv (\boldsymbol{u}_{\tau,i} - \boldsymbol{u}_{T,ign,i})/\boldsymbol{u}_{\tau,i}$ for the *i*th component.

As shown, the relative errors are within 5% for the top 16 reactions, and become larger for the small component as the numerical error for the insensitive reactions using the finite difference approach is larger. Such numerical error can be reduced by using an adaptive perturbation factor for those insensitive reactions in the finite difference approach. However, since most of the sensitivity analysis is motivated to the sensitive reactions, we did not further refine the perturbation factor.

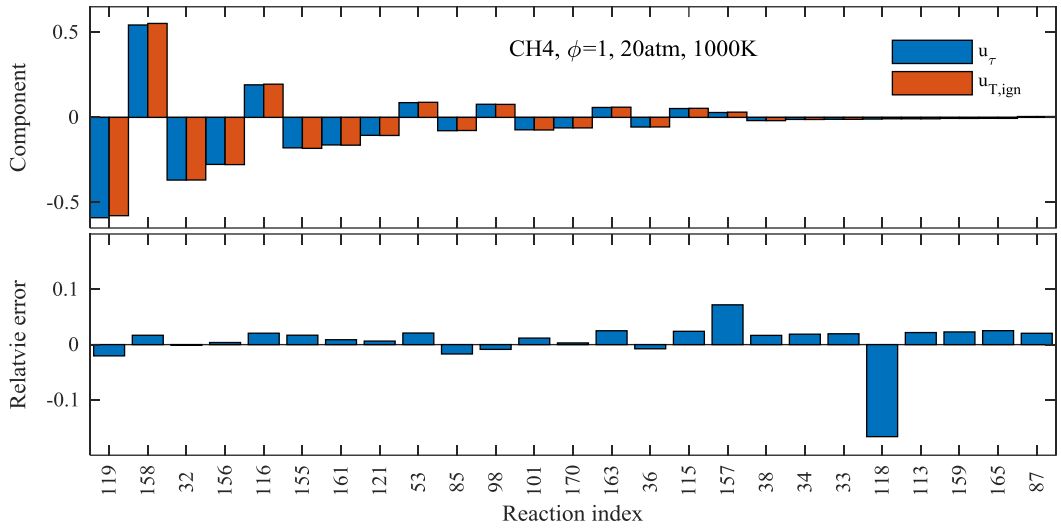

Fig. 5. Components of the sensitivity direction for IDT and the component-wise relative differences between $\boldsymbol{u_\tau}$ and $\boldsymbol{u_{T,ign}}$.

Such excellent alignment can be explained by Fig. 6, in which the rate constant for R119, the most sensitive reaction for IDT, is increased by 0.005% and leads to a shorter IDT. According to the triangle in Fig. 6, we have

$$\frac{\partial \tau}{\partial k_i} = \frac{\partial \tau}{\partial T}\frac{\partial T}{\partial k_i} = \frac{\Delta \tau}{\Delta T}\frac{\Delta T}{\Delta k_i} \tag{6}$$

Equation (6) implicitly assumes that the changes of $\frac{\partial \tau}{\partial T}$ at the ignition state is insignificant compared to the change of temperature, $\frac{\partial T}{\partial k_i}$. The term $\frac{\partial \tau}{\partial T}$ is inversely proportional to the rate-of-change of temperature and thereafter the heat release rate at the ignition state. The term $\frac{\partial T}{\partial k_i}$ is attributed to the accumulated sensitivity during the entire ignition delay period. The assumption for Eq. (6) is justified by the analysis in Sec. 2, in that the evolving of the autoignition trajectory near the ignition state is not sensitive to those rate-limiting steps for the induction period. Note that the correlation between the normalized sensitivity can be readily derived from Eq. (6).

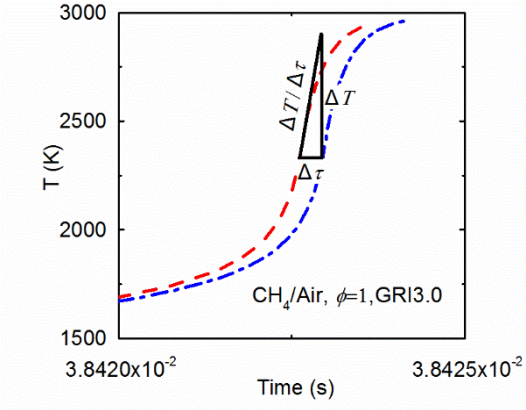

Fig. 6. Relations between changes of the ignition delay τ and temperature at ignition due to perturbation of the rate constant.

The correlation of Eq. (6) is further validated against the results from the finite difference approach for the autoignition process of various fuels, covering both fuel-lean and fuel-rich conditions, across a wide range of pressures and temperatures as listed in Table 1. Typical results for DME, *n*-heptane and *iso*-octane are provided in the supplemental material. The inner product between the directions of the sensitivity for IDT and the temperature sensitivity at ignition is always larger than 0.99 for all of the cases listed in Table 1. It is worth mentioning that the correlation is also valid for the first stage ignition delay time, as long as the two-stage ignition behavior can be clearly identified. Otherwise, it might show large difference due to the large uncertainty in determining the ignition state for the first stage ignition.

In addition to the constant volume simulation, the correlation is also validated in a simplified zero-D HCCI simulation with the configurations based on the experiments and simulations in [27]. Specifically, the engine speed is 1000 rpm; compression ratio (CR) is 16.5; piston diameter and stroke length are 12.065 cm and 14.005 cm, respectively; ratio of the length of the engine connecting rod to the crank radius (LOLR) is 3.71; and the inlet valve close crank angle (IVC) is 142° BTDC. The initial mixture is natural gas in air; the composition by volume are CH_4:0.0350, C_2H_6:0.0018, C_3H_8:0.0012,

O_2:0.1824, CO_2:0.0326, H_2O:0.0609, N_2:0.6861; and the initial temperature and pressure at IVC are 447 K and 1.065 atm respectively. The mechanism employed is GRI3.0 [18]. The inner product between the sensitivity direction for the ignition delay time (crank angle) and the temperature sensitivity at ignition is larger than 0.999. The components of the sensitivity directions and the component-wise difference between $\boldsymbol{u}_\tau$ and $\boldsymbol{u}_{T,ign}$ are further shown in Fig. 7. Similar to the case of methane in Fig. 5, the relative differences are within 5% for the top ten components.

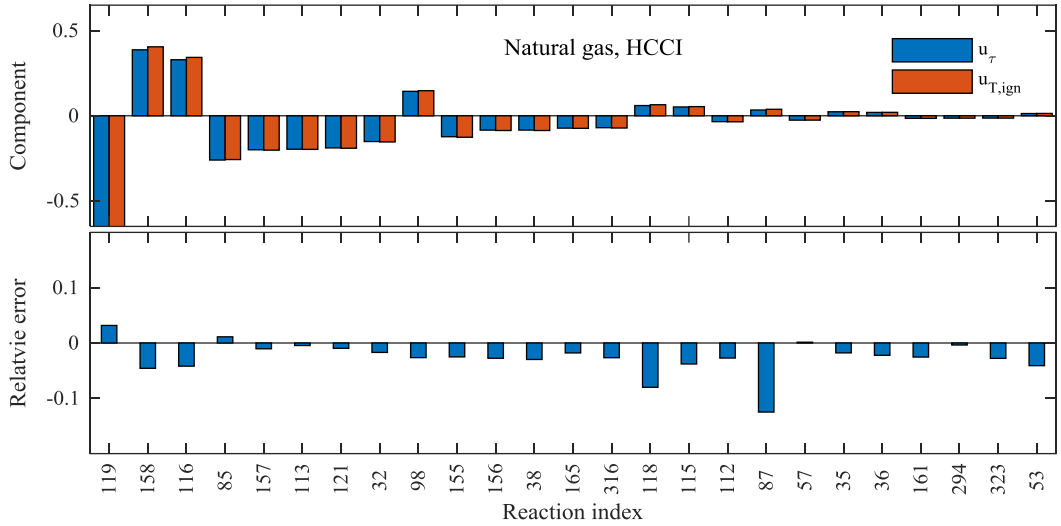

Fig. 7 Components of the sensitivity direction for IDT in the HCCI case and the component-wise relative differences between $\boldsymbol{u}_\tau$ and $\boldsymbol{u}_{T,ign}$.

Based on the correlation of Eq. (6), we can determine the sensitivity of IDT from the temperature sensitivity at ignition. However, it is challenging to accurately determine the proportionality constant via the temporal derivative of temperature as it changes sharply at ignition. Instead, we propose the following procedure: first calculate the local temperature sensitivity at ignition with one run of autoignition integration, and then calculate the sensitivity of IDT to the highest sensitive reaction in $\boldsymbol{u}_{T,ign}$ using the finite difference approach, denoted as $\frac{\partial \ln \tau}{\partial \ln k_j}$. Then the sensitivity of IDT to the rest of reactions is given by

$$\frac{\partial \ln \tau}{\partial \ln k_i} \Big/ \frac{\partial \ln \tau}{\partial \ln k_j} = \frac{\partial \ln T}{\partial \ln k_i} \Big/ \frac{\partial \ln T}{\partial \ln k_j} \tag{7}$$

The finite difference approach on the most sensitive reaction k_j is used to estimate the ratio between the sensitivity of IDT and the temperature sensitivity. The most sensitive reaction is chosen to avoid the discretization error when a small perturbation factor is used. If only the relative sensitivity is desired, the sensitivity direction is sufficient and the estimation of the ratio can be omitted.

Conclusions

We have studied the time evolution of the composition sensitivity during autoignition. The similarity among the sensitivity vectors studied in [3] is extended to the two-stage ignition, i.e., the sensitivity directions of temperature and most of the intermediate species concentration are similar to each other during the ignition delay period, and consequently converge to the same direction when approaching ignition during both the first-stage and second-stage ignition. An explanation based on the attracting manifold and its sensitivity is presented. Specifically, the sensitivity of the attracting manifold vanishes when approaching equilibrium, and the sensitivity of the autoignition trajectory is parallel to the intrinsic low-dimensional manifold (ILDM) when approaching ignition.

Furthermore, it is found that the sensitivity of the ignition delay time is proportional to the temperature (and species concentrations) sensitivity. The correlation is validated using various fuels, including methane, DME, *n*-heptane, and *iso*-octane, under both fuel-lean and fuel-rich conditions, covering both single-stage and two-stage ignition. In addition to the constant volume and constant pressure simulations, the correlation is also validated in zero-D HCCI simulation. The inner product between the sensitivity direction of the ignition delay time and the temperature sensitivity direction at the ignition state is always larger than 0.99 under all the test cases. We then proposed an efficient approach to compute the sensitivity of the ignition delay time from the temperature sensitivity. The approach only requires two auto-ignition integrations while the number of runs required by the conventional finite difference approach is proportional to the number of parameters. This approach

suggests extensive opportunities for efficiently optimizing large reaction mechanism using gradient-based algorithms.

Recognizing that the similar behavior has been studied in the laminar freely propagated premixed flames in the suggested works [3], i.e., the similarity between the sensitivity vectors of the compositions and the laminar flame speed, the current work found analogous behavior in the auto-ignition system, and will help build a more comprehensive picture of the similarity in homogenous auto-ignition and one-d flame system.

Acknowledgments

This work was supported by the National Natural Science Foundation of China No. 91441202.

References

[1] T. Turányi, Reliab. Eng. Syst. Safe., 57 (1997) 41-48.
[2] S. Vajda, P. Valko, T. Turanyi, Int. J. Chem. Kinet., 17 (1985) 55-81.
[3] I.G. Zsely, J. Zador, T. Turanyi, The Journal of Physical Chemistry A, 107 (2003) 2216-2238.
[4] J. Zádor, I.G. Zsély, T. Turányi, Int. J. Chem. Kinet., 36 (2004) 238-252.
[5] I.G. Zsély, T. Turányi, PCCP, 5 (2003) 3622-3631.
[6] I.G. Zsély, J. Zádor, T. Turányi, Combust Theor Model, 9 (2005).
[7] T. Turányi, A.S. Tomlin, Similarity of Sensitivity Functions, in: Analysis of Kinetic Reaction Mechanisms, Springer, Berlin, Heidelberg, 2014, pp. 313-335.
[8] A. Lovrics, A. Csikász-Nagy, I.G. Zsély, J. Zádor, T. Turányi, B. Novák, BMC Bioinformatics, 7 (2006) 494.
[9] A.E. Lutz, R.J. Kee, J.A. Miller, SENKIN: A FORTRAN program for predicting homogeneous gas phase chemical kinetics with sensitivity analysis, Report No. SAND-87-8248, Sandia National Labs., Livermore, CA (USA), 1988.
[10] D.G. Goodwin, H.K. Moffat, R.L. Speth, available at <http://www.cantera.org>.
[11] K. Braman, T.A. Oliver, V. Raman, Combust. Theor. Model., 19 (2015) 29-56.
[12] H. Wang, D.A. Sheen, Prog. Energy Combust. Sci., 47 (2015) 1-31.
[13] M. Frenklach, H. Wang, M.J. Rabinowitz, Prog. Energy Combust. Sci., 18 (1992) 47-73.
[14] W. Ji, J. Wang, O. Zahm, Y.M. Marzouk, B. Yang, Z. Ren, C.K. Law, Combust. Flame, (2017 in press).
[15] É. Hébrard, A.S. Tomlin, R. Bounaceur, F. Battin-Leclerc, Proc. Combust. Inst., 35 (2015) 607-616.
[16] P.G. Constantine, E. Dow, Q. Wang, SIAM J. Sci. Comput, 36 (2014) A1500-A1524.
[17] T.M. Russi, Uncertainty Quantification with Experimental Data and Complex System Models, PhD Thesis, UC Berkeley,California,USA, 2010
[18] Gregory P. Smith, David M. Golden, Michael Frenklach, Nigel W. Moriarty, Boris Eiteneer, Mikhail Goldenberg, C. Thomas Bowman, Ronald K. Hanson, Soonho Song, J. William C. Gardiner,

Vitali V. Lissianski, Z. Qin, available at <http://www.me.berkeley.edu/gri_mech/>.
[19] Z. Zhao, M. Chaos, A. Kazakov, F.L. Dryer, Int. J. Chem. Kinet., 40 (2008) 1-18.
[20] C.S. Yoo, T. Lu, J.H. Chen, C.K. Law, Combust. Flame, 158 (2011) 1727-1741.
[21] C.S. Yoo, Z. Luo, T. Lu, H. Kim, J.H. Chen, Proc. Combust. Inst., 34 (2013) 2985-2993.
[22] S.S. Merchant, C.F. Goldsmith, A.G. Vandeputte, M.P. Burke, S.J. Klippenstein, W.H. Green, Combust. Flame, 162 (2015) 3658-3673.
[23] K. König, U. Maas, Proc. Combust. Inst., 30 (2005) 1317-1323.
[24] J. Huang, P. Hill, W. Bushe, S. Munshi, Combust. Flame, 136 (2004) 25-42.
[25] W. Ji, P. Zhao, P. Zhang, Z. Ren, X. He, C.K. Law, Proc. Combust. Inst., 36 (2016) 343-353.
[26] N. Peters, G. Paczko, R. Seiser, K. Seshadri, Combust. Flame, 128 (2002) 38-59.
[27] M. Christensen, B. Johansson, P. Amnéus, F. Mauss, Supercharged Homogeneous Charge Compression Ignition, SAE International, 1998.

Tables and figure captions

Table 1. Chemical mechanisms and conditions for autoignition processes

Fuel/mech	No. species	No. reactions	ϕ	p [atm]	T [K]
Methane (CH_4) [18]	53	325	0.5, 1, 2	1, 20	1000-1500
DME (CH_3OCH_3) [19]	55	290	0.5, 1, 2	1, 20	1000-1500
n-heptane (*n*-C_7H_{16}) [20]	88	729	0.5, 1, 2	1, 20	600-1500
iso-octane (*i*-C_8H_{18}) [21]	143	1178	0.5, 1, 2	1, 20	600-1500

Fig. 1. Evolution of temperature, its rate of change, and the magnitude of its sensitivity vector to kinetic parameters against the normalized time. The unit of dT/dt is K/s. The IDT is 38.4 ms in (a) and 0.7 ms in (b).

Fig. 2. Evolutions of the inner product (absolute value) between the sensitivity directions of composition and $\boldsymbol{u}_{T,ign}$.

Fig. 3. The most sensitive reactions for temperature at the ignition point.

Fig. 4 Evolution of the most sensitive reactions for temperature.

Fig. 5. Components of the sensitivity direction for IDT and the component-wise relative differences between $\boldsymbol{u}_{\tau}$ and $\boldsymbol{u}_{T,ign}$.

Fig. 6. Relations between changes of the ignition delay τ and temperature at ignition due to perturbation of the rate constant.

Fig. 7 Components of the sensitivity direction for IDT in the HCCI case and the component-wise relative differences between $\boldsymbol{u}_{\tau}$ and $\boldsymbol{u}_{T,ign}$.